AGU PUBLICATIONS

JGR

Journal of Geophysical Research: Atmospheres

RESEARCH ARTICLE
10.1002/2017JD027379

Key Points:
- Our calibration and validation demonstrate that the General Lake Model is suited for the thermal simulation of lakes on the Tibetan Plateau
- The epilimnion of Nam Co has warmed, whereas the onset of summer stratification has advanced and its duration has increased during 1979–2012
- Increased air temperature and downward longwave radiation are two driving factors responsible for the warming of Nam Co

Supporting Information:
- Supporting Information S1
- Data Set S1
- Data Set S2
- Data Set S3
- Data Set S4
- Data Set S5

Correspondence to:
J. Wang,
wangjb@itpcas.ac.cn

Citation:
Huang, L., Wang, J., Zhu, L., Ju, J., & Daut, G. (2017). The warming of large lakes on the Tibetan Plateau: Evidence from a lake model simulation of Nam Co, China, during 1979–2012. *Journal of Geophysical Research: Atmospheres*, *122*, 13,095–13,107. https://doi.org/10.1002/2017JD027379

Received 29 JUN 2017
Accepted 12 NOV 2017
Accepted article online 16 NOV 2017
Published online 19 DEC 2017

The Warming of Large Lakes on the Tibetan Plateau: Evidence From a Lake Model Simulation of Nam Co, China, During 1979–2012

Lei Huang[1,3], Junbo Wang[1,2], Liping Zhu[1,2], Jianting Ju[1], and Gerhard Daut[4]

[1]Key Laboratory of Tibetan Environment Changes and Land Surface Processes (TEL), Institute of Tibetan Plateau Research, Chinese Academy of Sciences, Beijing, China, [2]CAS Center for Excellence in Tibetan Plateau Earth Sciences, Beijing, China, [3]University of Chinese Academy of Sciences, Beijing, China, [4]Physical Geography, Institute of Geography, Friedrich-Schiller-University Jena, Jena, Germany

Abstract Lakes are considered as indicators of climate change on the Tibetan Plateau (TP). In the present study, we use the General Lake Model to simulate water temperature changes in Nam Co, the second largest lake on the central TP, for the period 1979–2012. The calibration and validation results demonstrate that this model is well suited for thermal simulation of Nam Co. The simulation results indicate that Nam Co has responded to the recent warming climate. The average summer surface water temperature fluctuated yearly, but its trend is positive at a rate of 0.52 ± 0.25°C per decade. At the same time, the onset of summer stratification advanced by 4.20 ± 2.02 d per decade, and the duration increased at a rate of 6.00 ± 3.54 d per decade. To explore the roles of air temperature and longwave radiation in lake warming, three sensitivity experiments are conducted by removing long-term trends from time series of air temperature and longwave radiation in the forcing data. These experiments prove that both increased air temperature and downward longwave radiation are two driving factors responsible for the warming of Nam Co.

1. Introduction

Global warming has been widely discussed in recent decades. Studies show high rates of warming for both the air over land (0.254 ± 0.050°C per decade, 1979–2012) and sea surface water (0.124 ± 0.030°C per decade, 1979–2012) during the twentieth century, especially within the last four decades (Hartmann et al., 2013). Lakes hold a large proportion of Earth's liquid water and have a near-global distribution. They are sensitive to and are considered to be sentinels of climate change (Adrian et al., 2009; Schindler, 2009). A recently published, global database of lake surface temperatures shows that 235 globally distributed lakes are warming significantly, with a mean increasing trend of 0.34°C per decade between 1985 and 2009 (O'Reilly et al., 2015; Sharma et al., 2015). Similar observed warming rates between land surface air temperatures and lake surface temperatures may indicate a close relationship between them (Schmid et al., 2014; Schneider & Hook, 2010). Besides the warming of lakes' surface water, several further responses have also been widely detected, such as more stable stratification, shorter periods of ice cover and shallower thermocline depths (Adrian et al., 2009; Arhonditsis et al., 2004; Coats et al., 2006; Shimoda et al., 2011). Ecologists argue that changes in water temperatures can directly or indirectly affect the physiology, distribution, and life cycles of aquatic organisms in lakes, as well as the food web in these environments (Arhonditsis et al., 2004; Arvola et al., 2010; Coats et al., 2006; Hampton et al., 2008; Shimoda et al., 2011).

Lake surface warming is globally observed, but the warming rates are quite spatially heterogeneous with no rigid regional coherence (O'Reilly et al., 2015). Especially, in many remote areas, only a few long-term lake monitoring records exist (Sharma et al., 2015). Model simulations could be an alternative method to investigate lake water temperature changes (Janssen et al., 2015). Lake water temperatures can be well simulated by hydrodynamic models even through decadal time scales (Coats et al., 2006; MacKay et al., 2009; Peeters et al., 2002). General Lake Model (GLM) is a one-dimensional hydrodynamic model for simulating water balance and vertical stratification of lakes which was developed based on the approach used within the Dynamic Reservoir Simulation Model (Hipsey et al., 2014). The reliability of this approach simulating lake water temperatures on decadal timescale has been validated by observational data (Coats et al., 2006; Perroud et al., 2009; Tanentzap et al., 2007). Coupled with a snow-ice module the GLM can simulate water temperatures of lakes under different climate conditions including seasonally ice-covered lakes as well as ice-free lakes (Hipsey et al., 2014; Read et al., 2014; Yao et al., 2014).

The Tibetan Plateau (TP) is experiencing rapid warming, which is associated with changes in the hydrological cycle (Immerzeel et al., 2010; Kuang & Jiao, 2016). The rate of increase of air temperature on the TP during 1984–2009 was 0.46°C per decade, based on observational data (Kuang & Jiao, 2016). This rate is greater than the rate of change of global land surface air temperature over a similar period (1979–2012) (Hartmann et al., 2013). There are more than 1,000 lakes with lake area over 1 km^2 on the TP. These lakes are sensitive indicators of climate change and react via changes in water levels, water volumes, and lake ice phenology (Ke et al., 2013; Liu et al., 2009; Yang et al., 2017; Zhang, Yao, Xie, Qin, et al., 2014; Zhang, Yao, Xie, Zhang, et al., 2014). In contrast to other lake areas, only a few studies have focused on changes in the thermal characteristics of lakes in response to global warming on the TP (Zhang, Yao, Xie, Qin, et al., 2014). Zhang, Yao, Xie, Qin, et al. (2014) used Moderate Resolution Imaging Spectroradiometer (MODIS) LST (LST = Lake surface temperature) data between 2001 and 2012 to reconstruct lake surface temperatures and found that 31 of 52 investigated lakes displayed a temperature increase during 2001–2012 on the TP, and some lakes warmed more rapidly than the ambient air. This research only discussed lake surface temperatures without discussion on thermal changes inside the water body, and the MODIS LST data were not solidly validated since a limited amount of in situ measured water temperature data.

Here we present a model (GLM) simulation of Nam Co to ascertain characteristics of lake warming and its heat budget drivers. This model has first been calibrated and validated using in situ temperature measurements and a MODIS LST product. By using corrected meteorological reanalysis data, daily water temperatures get simulated at all depths within Nam Co during 1979–2012. Linear trends in thermal changes that have occurred within Nam Co, such as in surface and bottom water temperatures, the depth of the thermocline, and the duration of stratification, are calculated. At last, we adopt a statistic method to quantitatively examine the individual role of air temperature and longwave radiation in lake warming.

2. Study Site

The surface area of Nam Co was 2,026 km^2 in 2010, and it is presently expanding (Zhang, Yao, Xie, Zhang, et al., 2014). The drainage area of Nam Co is approximately 10,680 km^2 (Zhou et al., 2013). Nam Co occupies a closed basin, and there is no surface outflow. Water balance observations show that runoff from unglaciated areas account for 55–65% of the total water input, whereas precipitation and meltwater inflow account for 23–28% and 7–22%, respectively (Zhou et al., 2013). Nam Co has a central basin with water depths of ~100 m (Figure 1), and the lake's volume was 86.4 km^3 in 2004. Nam Co is a slightly saline carbonate lake with an electrical conductivity of 1,851 μS/cm, on average (Wang et al., 2009). Surface water temperatures reach up to 12°C (daily average) in summer. Observations reveal that this lake stratifies from June to November, and the whole water column mixes during winter in the central part (Huang et al., 2015). It is generally ice covered from January or February to April or May (Ke et al., 2013; Qu et al., 2012). During the periods of ice cover that occurred in 2011–2013, the water temperature of the entire column dropped to nearly 0°C, and slightly inverted stratification can be observed, according to our measurements.

A monitoring station maintained by the Chinese Academy of Sciences is situated 1.5 km away from the south bank of Nam Co (Figure 1). It provides common meteorological data that are accessible from the Third Pole Environment data center (DOI: 10.11888/AtmosphericPhysics.tpe.249300.db). The data show that the Indian Ocean Summer Monsoon controls the summer climate in the Nam Co area, whereas the Westerlies control the winter climate. The annual mean air temperature was −0.56°C during 2006–2008 with February as the coldest month and July as the warmest month. The annual precipitation was approximately 415 mm during this period; most of the precipitation falls during the summer (monsoon) season. The annual mean wind speed is 3.54 m/s, and strong winds commonly occur during wintertime.

3. Method and Data

3.1. The General Lake Model

The General Lake Model (Hipsey et al., 2014) adopts a one-dimensional solution scheme for vertical mixing by incorporating a flexible Lagrangian layer structure. The water balance is composed of surface mass fluxes, inflows, and outflows. The lake surface energy budget is determined by the balance of shortwave and longwave radiation fluxes, as well as sensible and evaporative heat fluxes. GLM also contains an ice model that employs a quasi-steady heat transfer equation. It is ideally suited to interannual and decadal simulations

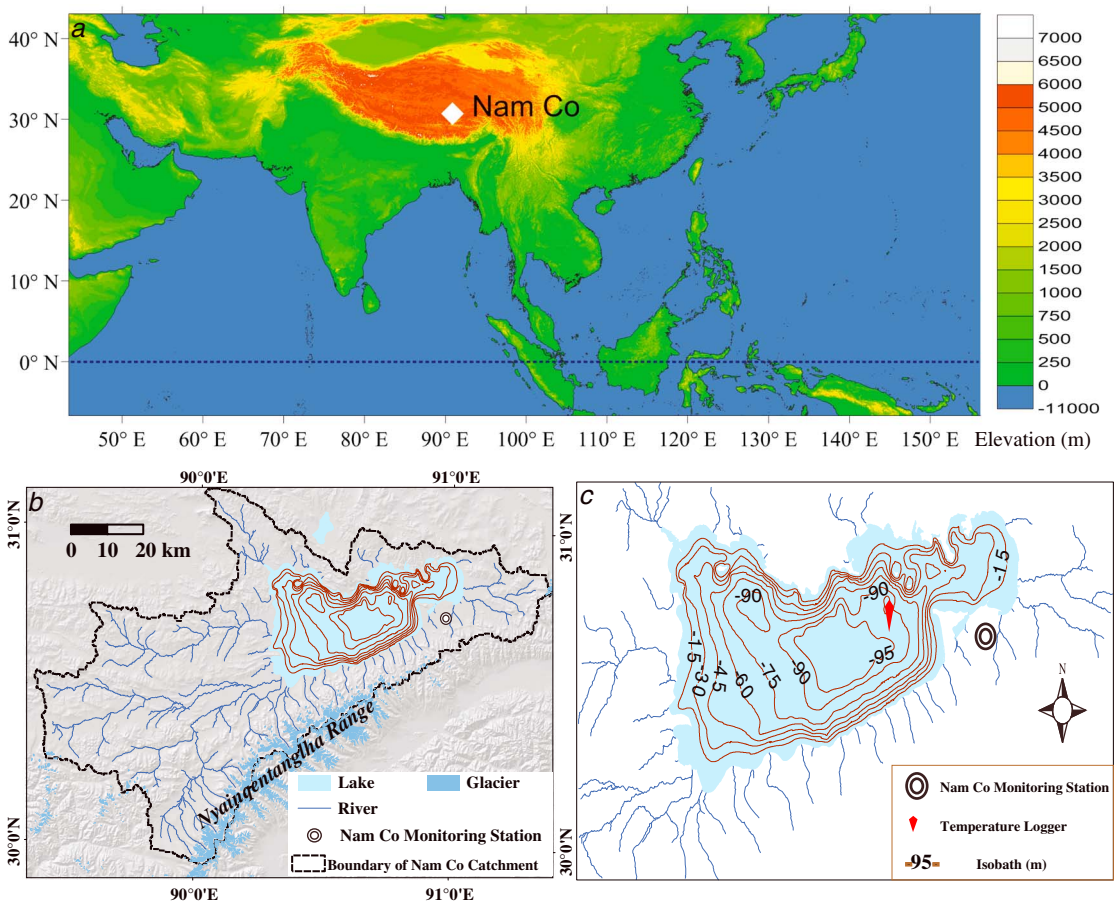

Figure 1. (a) Elevation model showing the location of Nam Co on the TP, (b) map showing Nam Co with its catchment area, including rivers and glaciers, and (c) a bathymetric map of Nam Co showing the locations of temperature logging stations on the lake.

for deep and stratified lakes. The required meteorological input data include daily shortwave and longwave radiation, air temperature, relative humidity, wind speed, and precipitation. Version 2.2.0 of GLM (Hipsey et al., 2014) is used in this research. The output of GLM includes water temperatures for the whole water column and surface heat fluxes.

3.2. Water Temperature Observations and MODIS LST Product

Water temperatures have been recorded during 2011–2014 at several depths (6, 16, 21, 31, 56, and 66 m) by Vemco Minilog-II-T Temperature Data Loggers every 10 min in the central part of Nam Co (30°46.076′N, 90°46.529′E, 92 m deep) (Figure 1). By deploying two Sea&Sun Marine Tech CTD 90 M Multiparameter Probes on the same profile, additional temperature data were collected at depths of 3 and 83 m at a 2 h interval during 2012–2013. To calibrate the model, water temperatures at all depths are averaged daily. The thermocline depth during stratification is calculated by the method of Read et al. (2011). During mixing periods, it is set to the maximum value, for example, 83 m.

To further validate the simulation results, a lake surface temperature data set covering 2000–2014 retrieved from a MODIS LST product (MOD11A1) was applied (Savtchenko et al., 2004). This product includes one instantaneous observation (Day_LST) at 11:00 and another one (Night_LST) at 21:00 (local time) every day, both of which were used (Lazhu et al., 2016). Values lower than 0°C are abandoned because there are no observations lower than 0°C.

3.3. Meteorological and the ITPCAS Forcing Data

The GLM is driven by daily time series of meteorological data such as air temperature, shortwave radiation, and wind speed. Daily air temperature, wind speed, relative humidity, precipitation, and global solar

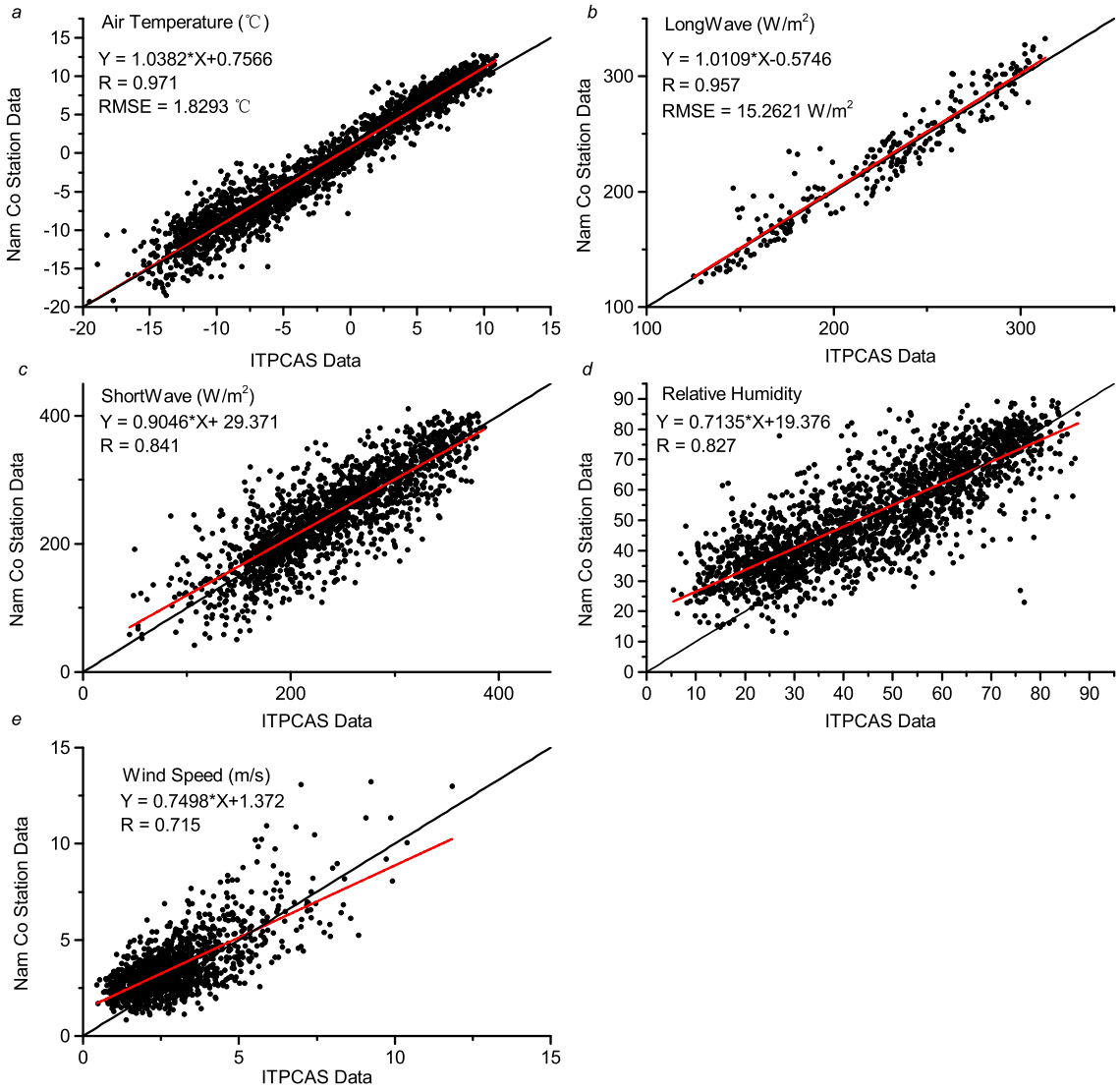

Figure 2. Statistical correlation parameters of observed meteorological data at Nam Co station and ITPCAS forcing data from 2005 to 2012: (a) air temperature; (b) downward longwave radiation; (c) downward shortwave radiation; (d) relative humidity; and (e) wind speed. Black lines indicate 1:1 lines; red lines indicate best fit lines.

radiation data recorded by Vaisala automatic weather stations at the Nam Co monitoring station cover the period from 2005 to 2015. Downward shortwave and longwave radiation are only available in 2012, and these data were recorded by a Vaisala PBL tower.

A China regional surface meteorological feature data set (He, 2010) developed by Data Assimilation and Modeling Center for Tibetan Multispheres, the Institute of Tibetan Plateau Research, Chinese Academy of Sciences (hereafter ITPCAS) is used as atmospheric forcing data for the GLM. This data set is accessible in the Third Pole Environment Database (http://en.tpedatabase.cn/portal/). It has been widely used in research on hydrological changes because observed meteorological data are rare or of poor quality in most areas on the TP (Chen et al., 2011; Yang et al., 2010). The version used here covers the period of 1979–2012 with a spatial resolution of 0.1° × 0.1° and a temporal resolution of 3 h. The 740 China Meteorological Administration (hereafter CMA) stations' observational data are merged into the corresponding Princeton meteorological forcing data (Sheffield et al., 2006) to produce the near-surface air temperature, pressure, wind speed, and specific humidity. The downward shortwave radiation is constructed by correcting the Global Energy and Water Cycle Experiment-Surface Radiation Budget shortwave radiation data set (Pinker & Laszlo, 1992), with reference to radiation estimates from meteorological station data using a hybrid radiation model. The

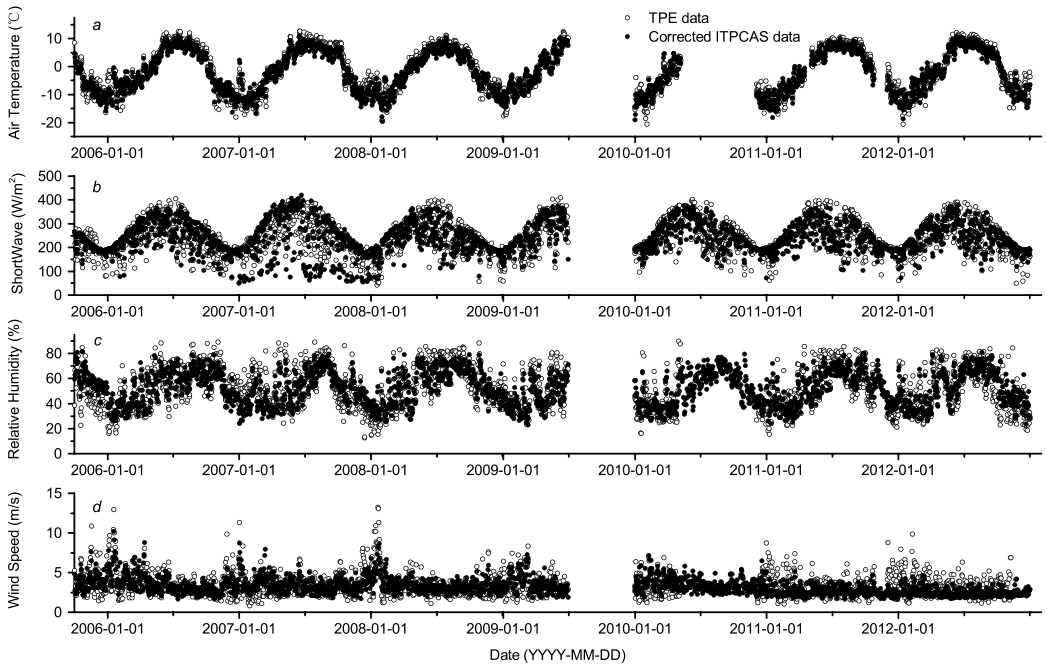

Figure 3. Comparison of observed and corrected data: (a) air temperature; (b) downward shortwave radiation; (c) relative humidity; and (d) wind speed.

produced near-surface air temperature, pressure, specific humidity, and downward shortwave radiation are used to drive Crawford and Duchon's (1999) model to produce downward longwave radiation.

First, we retrieve air temperature and specific humidity values at 2 m above the land surface, wind speed at a height of 10 m, surface pressure, precipitation, and downward shortwave and longwave radiation from the ITPCAS data set. The specific humidity data are then converted to relative humidity, based on equation (1).

$$\mathrm{Rh} = 100\times\frac{\omega}{\omega_s}\approx 0.263pq\left[\exp\left(\frac{17.67(T-T_0)}{T-29.65}\right)\right]^{-1} \quad (1)$$

where Rh is relative humidity, ω is the mass mixing ratio of water vapor to dry air, ω_s is the mass mixing ratio of water vapor to dry air at equilibrium, p is the air pressure in hPa, q is the specific humidity, T is the air temperature in K and T_0 is 273.16 K.

Because meteorological stations on the TP are sparse, biases between the ITPCAS forcing data and the observations collected at the Nam Co monitoring station may exist. To improve the accuracy of the simulation, correction of the ITPCAS forcing data is necessary. Comparisons between the observational data and the ITPCAS

Table 1
Calibration Details

		Initial value	Minimum acceptable value	Maximum acceptable value	Calibration results
Shortwave factor		1	0.9	1.1	0.96266
Longwave factor		1	0.8	1.2	0.95228
Wind speed factor		1	0.9	1.1	0.95311
Air temperature factor		1	0.8	1.2	0.94934
Relative humidity factor		1	0.8	1.2	1.011
Extinction coefficient		0.1028	0.07	0.15	0.10017
Mixing parameters	Convective overturning	0.125	0.1	0.2	0.12418
	Wind stirring	0.23	0.2	0.3	0.22666
	Shear production	0.2	0.15	0.25	0.20922
	Unsteady turbulence	0.51	0.45	0.56	0.51679
	Kelvin-Helmholtz turbulent billows	0.3	0.25	0.35	0.2675
	Hypolimnetic turbulence	0.5	0.45	0.55	0.51716

Note. Initial values represent the defaults in GLM (Hipsey et al., 2014), except for the extinction coefficient, convective overturning, and shear production.

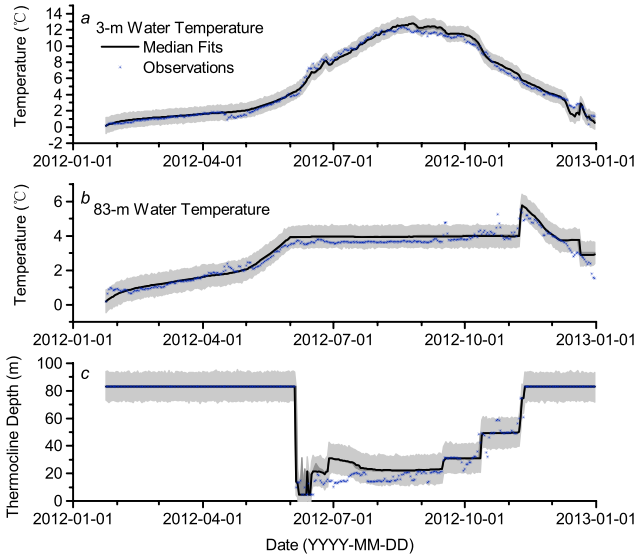

Figure 4. Calibration of mixing parameters. Dark gray areas correspond to the 95% posterior limits of the model uncertainty due to parameters, and lighter areas give the 95% posterior uncertainty in predicting new observations. Black lines are the median fits obtained from MCMC calibration, and blue dots represent measured data.

forcing data are made for the period 2005–2012. Linear regression analysis is employed, and the empirical relationships are used to correct the ITPCAS data to produce a continuous time series of meteorological data during 1979–2012.

As Figure 2 shows, the ITPCAS forcing data display good agreement with the observations from 2005 to 2012. Air temperature (Figure 2a) has the highest coefficient of correlation (R =0.971) and a small root-mean-square error (RMSE = 1.829°C). The slope of a linear fit between the observations and the forcing data is 1.038. The observational longwave radiation data (Figure 2b) are only available for 2012, but the observations and forcing data are very close, with a RMSE of only 15.262 W/m^2. The slope of the linear fit is 1.011. Air temperatures and longwave radiation in the ITPCAS forcing data are treated as observations and used directly as input data in the simulation. We also argue that the effects of precipitation on water temperature changes are not significant, considering the large water volume of Nam Co. Thus, the precipitation data are not corrected and are used directly. We use observations of global solar radiation during 2005–2012 to correct the shortwave radiation in the forcing data (Figure 2c). Based on linear regression analysis, the coefficient of correlation between them is 0.841. The shortwave radiation values in the ITPCAS forcing data are then corrected using this fitted linear relationship. The RMSE between the observations of global solar radiation and the corrected ITPCAS forcing data is 37.559 W/m^2 (Figure 3b). The same correction method is applied to relative humidity and wind speed. The correlation coefficient between the observations and the forcing data is 0.827 for relative humidity and 0.715 for wind speed, respectively. As Figure 3 shows, the RMSE for observed and corrected relative humidity is 9.320%; for wind speed, it is 1.083 m/s.

3.4. Configuration

The hypsographic curve for the lake basin is calculated using measured bathymetric data (Wang et al., 2009). Because no water input data are available during the simulation period (1979–2012), the number of inflowing streams is set to 0. Modern monitoring data show that inflowing streams amount to 810–1,200 mm of lake level increase (1.63–2.47 km^3) during summer (Zhou et al., 2013). Considering the large water volume of Nam Co (86.4 km^3), we argue that inflowing streams have limited influence on water temperature changes at the decadal time scale considered here. By using a Hydrolab-MS5 sonde with a PAR (photosynthetically active radiation) probe, we obtained four vertical PAR profiles in the central part of Nam Co. An average extinction coefficient (0.103) for PAR in these four profiles is applied in this research (Table 1). A recent study on this lake obtained a similar extinction coefficient (0.12–0.16 m^{-1}) for PAR (Nima et al., 2016). The lake ice module adopts the default parameter values (please see the configuration file in the supporting information).

The corrected ITPCAS forcing data are used to drive the GLM for the period of 1979–2012. Based on observations from 2011 to 2014, the whole water column mixed when surface water temperatures dropped to their lowest values in autumn/winter. Only minor differences in temperature are detected among different depths. Tests of GLM show that initial temperature profiles at the start of the year have a very slight influence on the simulation results at the end of the same year. Given these observations, we set the initial temperature for all depths on the first day of 1979 to 0.2°C. When the surface water temperature drops to the lowest value at the end of 1979, this point was set as the start of the simulation for 1980, and the lowest temperature at the end of 1979 was assigned to the initial temperature profile at all depths in 1980. The same method is repeated for every year of the simulation period (1979–2012). Afterward, a time series of simulated water temperatures through the last three decades at all depths was built. This discontinuous modeling approach neglects the carryover of heat stored in the lake from year to year. It is believed to be acceptable in other simulations of strictly dimictic lakes that freeze over each year (Peeters et al., 2002).

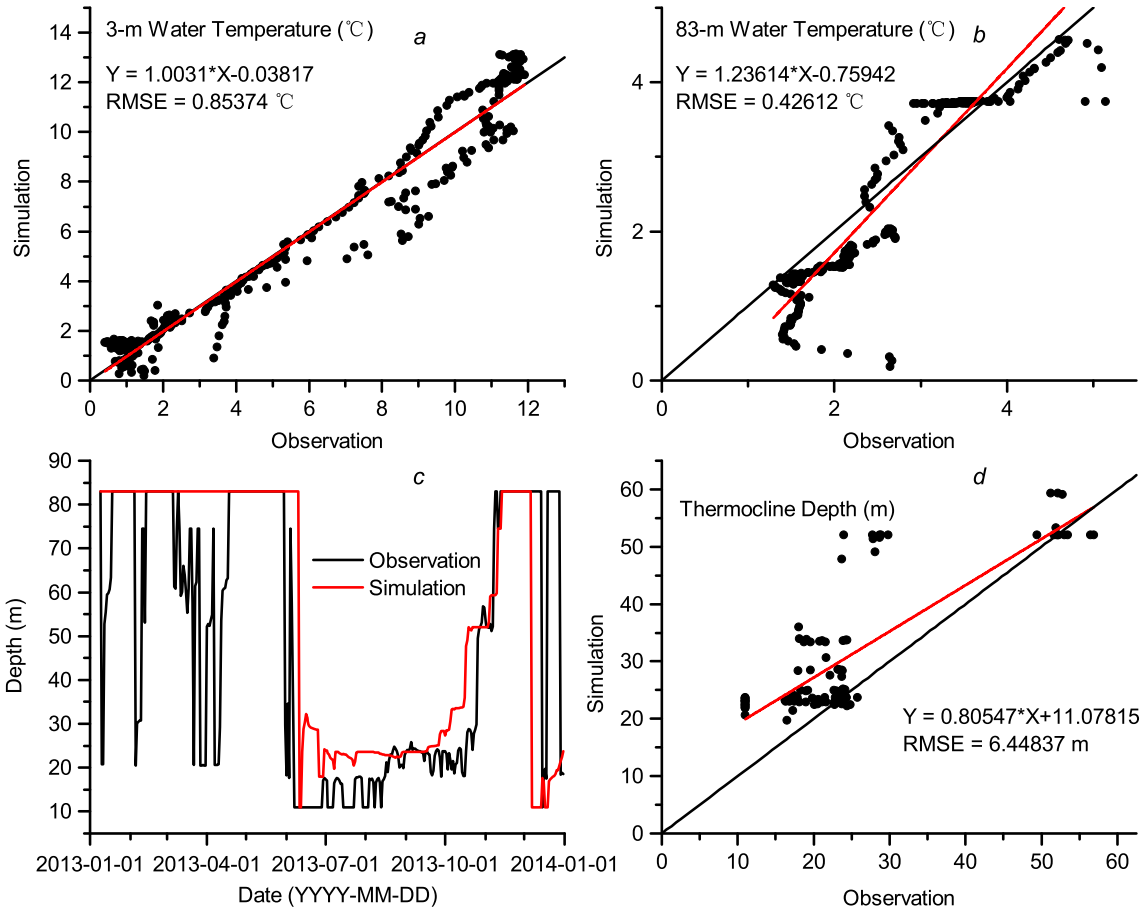

Figure 5. Validation of GLM in 2013. Linear regression analysis on simulated and observed water temperatures at (a) 3 m and (b) 83 m, as well as (d) thermocline depths in 2013; comparison between time series of (c) observed and simulated thermocline depths in 2013. Black straight lines indicate 1:1 lines; red straight lines indicate the linear fits between the simulation results and the observations.

3.5. Calibration

Water temperatures at depths of 3 m and 83 m, as well as the thermocline depth, are selected proxies to be calibrated. By utilizing the MCMC-DRAM (Markov chain Monte Carlo-Delayed Rejection and Adaptive Metropolis) method (Haario et al., 2006), the sum of squared deviations between the observations and the simulation results was used to process the calibration. Using the observational temperatures at 3 m in 2012, the shortwave, longwave, wind, air temperature, and relative humidity factors are calibrated first. Maximum and minimum values accepted for every factor are 1.1 and 0.9. Then, the mixing parameters and extinction coefficient were calibrated by using temperatures measured at depths of 3 m and 83 m, as well as the thermocline depth. The initial, maximum, and minimum values for each parameter are shown in Table 1. The calibration experiment was driven by observational meteorological data collected in 2012.

Figure 4 shows the variance of the predictive distribution. The very narrow predictive limits (darker gray areas) of the fitted model indicate a small uncertainty caused by mixing parameters. The 95% posterior uncertainty for new observations (lighter areas) covers most observation data which means this model can predict water temperatures and thermocline depths sufficiently well. The median (solid black lines, close to the best squares fit) estimated by MCMC method fits the observations closely, especially for water temperature at 3 m. From Figures 4b and 4c, some parts of lighter gray areas fail to cover the observations, this may be caused by internal oscillations of lakes in high frequency which are not simulated by the model. It should be noted that thermocline depths are set to 83 m during mixing periods in winter. So the rapid shifts of thermocline depths at the beginning and end of stratification are artificially made and they do not influence the calibration. The abrupt rising of 83 m water temperatures at the end of stratification is induced by overturning of the whole water column.

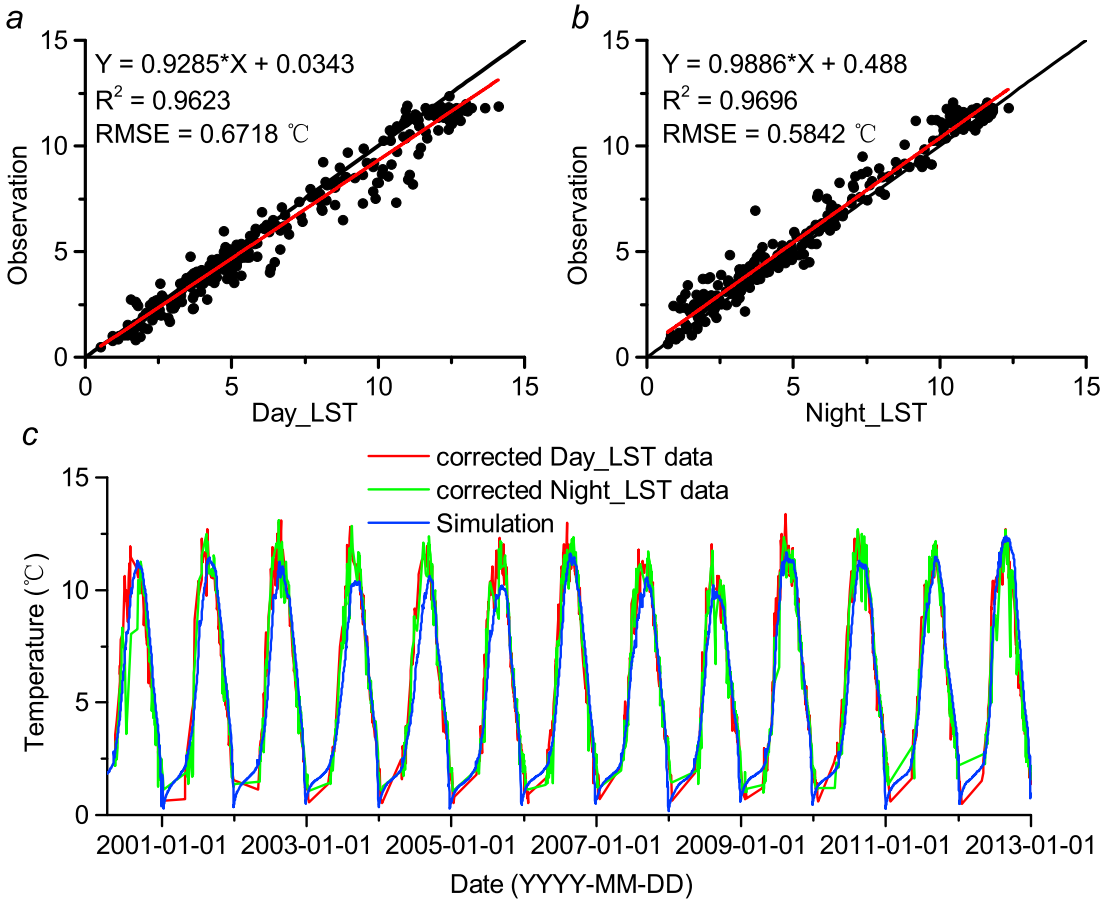

Figure 6. Validation of GLM based on MODIS LST. Linear regression analysis on MODIS LST and observed daily averaged water temperatures in 2011–2014: (a) Day_LST; (b) Night_LST; and (c) corrected MODIS LST and simulated surface water temperatures during 2000–2012. Black straight lines indicate 1:1 lines; red straight lines indicate the linear fits between MODIS LST and the observations.

3.6. Validation

To validate the simulation, its results were compared with observational data from 2013 (Figure 5). GLM simulates the surface layer temperatures well, and the RMSE is 0.854°C. The slope of the best fit line is 1.003, and the intercept is also close to 0. In summer, the simulated temperatures have larger deviations from the observations when the temperature is above 9°C. At a water depth of 83 m, the RMSE between simulated and observed water temperatures is 0.426°C. But the slope and intercept of the best fit line are larger than those of the surface layer. The annual variations in the thermocline depth are simulated well by GLM. The simulated thermocline depths, however, are larger than the observed values during stratification periods. The RMSE of the thermocline depths is 6.448 m during stratification periods (Figure 5d).

We also use MODIS LST data to validate the simulated surface water temperatures in 2000–2012 (Figure 6c). After quality control, the MODIS LST data are compared to the daily averaged observed surface water temperatures. This data set is highly reliable because it has a very strong linear correlation with the observations (Figure 6). Furthermore, it seems reasonable that Day_LST data are higher than the observations, whereas the Night_LST data are slightly lower than the observations, considering subdaily fluctuations in surface water temperatures. The correction method for the ITPCAS forcing data is also applied to the MODIS LST data. Comparison of the corrected Day_LST and Night_LST data with the simulated surface water temperatures confirms that the simulated data have values and variations that are very similar to those seen in the data. It should be noted that this comparison cannot be performed during the wintertime because MODIS data below 0°C are abandoned. Over the 12 year validation period, significant deviations appear only in 2003–2005. Therefore, we argue that for simulations over decadal time scales, GLM shows good performance with reliable results on lake water temperature changes from 1979 to 2012 that can be discussed further.

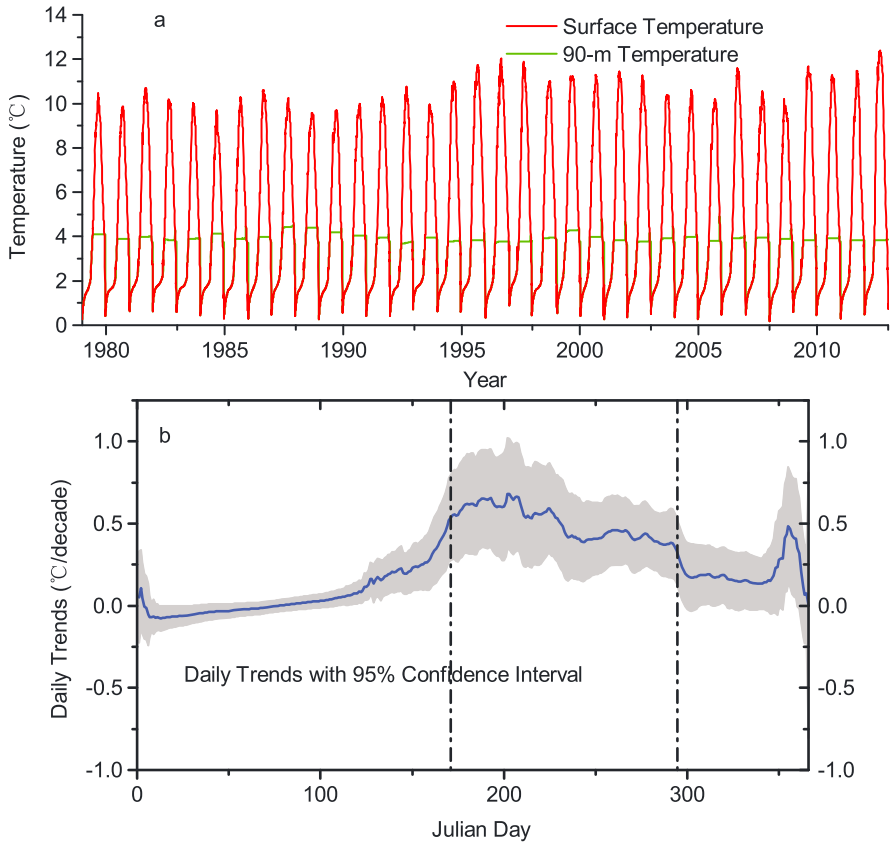

Figure 7. Simulated water temperature changes during the period 1979–2012: (a) simulated daily averaged water temperatures at the surface and 90 m depth; (b) daily trends (blue curve) with 95% confidence interval (shaded gray area) during 1979–2012. The two dashed vertical lines represent the boundaries of periods with high values that occur in summertime.

4. The Warming of Nam Co During 1979–2012

Figure 7a shows simulated daily water temperatures at the surface and at a depth of 90 m during 1979–2012. After validation, the changes in simulated water temperatures are examined. Linear regression analysis on the daily surface water temperature of each Julian day shows that surface water temperature increased most in the summertime, that is, July, August, and September (JAS), over the past 30 years (Figure 7b). Daily trends in JAS are larger than 0.1°C per decade and range up to 0.7°C per decade. In contrast, the winter season shows no clearly increasing trends in surface water temperature. Based on observations from 2011 to 2014, the temperatures of the whole water column are reset in winter and drop almost to 0°C. This resetting of temperatures may partly eliminate the increasing trend in winter and spring, even though the winter climate of the Tibetan Plateau has warmed during the last 30 years (Kuang & Jiao, 2016; You et al., 2010).

As Figure 7b shows, periods with high daily warming trends in surface water temperatures are approximately in accordance with periods of lake stratification. To further investigate the characteristics of water temperature changes in summer over successive years, average water temperatures in JAS are incorporated (Figure 8a). There is a clear increasing trend in surface water temperatures, and the slope is significantly different from 0 at the 0.05 confidence level. This increasing trend was 0.52 ± 0.25°C per decade ($p < 0.05$), and 2.5°C of temperature change occurred in total during 1979–2012. Water temperatures at a depth of 90 m, however, reflect no significant warming trend; instead, they even reflect a slight cooling (Figure 8b). It is possible that hypolimnion temperatures do not follow air temperature changes since heat transport from the surface to bottom is slow and always interrupted by internal oscillations. A worldwide synthesis of lake temperature data shows that the global mean increasing trend in summer surface water temperature is 0.34°C per decade during 1985–2009 (O'Reilly et al., 2015). While the epilimnion is experiencing warming, rarely available hypolimnion water temperature data, such as that from Lake Baikal and Lake Washington, show that the

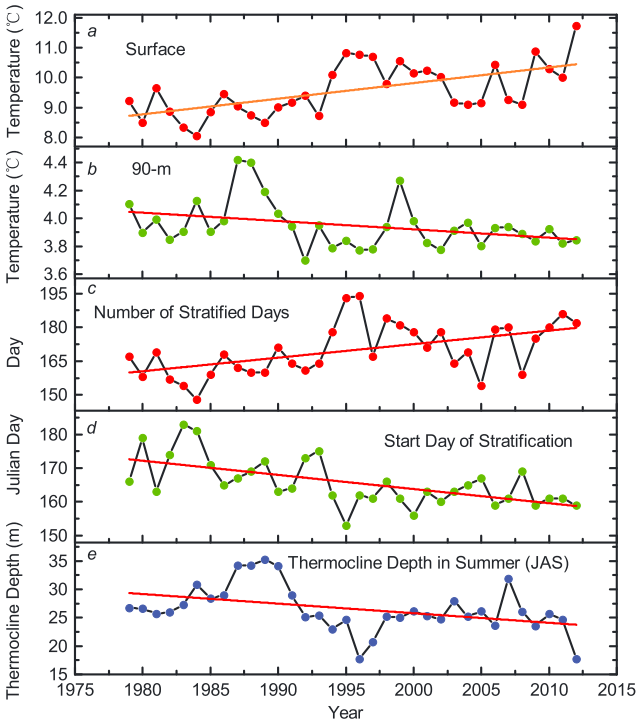

Figure 8. Thermal changes of Nam Co in summer (JAS) during 1979–2012. Average water temperatures of summer at the (a) surface and a depth of (b) 90 m, as well as the (c) number of stratified days, the (d) start day of stratification, and the (e) thermocline depth. Red lines represent best fit lines.

hypolimnion response is weaker than in the epilimnion (Arhonditsis et al., 2004; Arvola et al., 2010; Hampton et al., 2008; Shimoda et al., 2011). The hypolimnion of some northern temperate lakes has even cooled. The increased thermal stability due to the warming summer climate may be one reason for the observed hypolimnetic cooling (Arvola et al., 2010).

Lake warming can induce changes in thermodynamics and mixing regimes and thus influence lakes' biological systems. The simulation results show increasing numbers of stratified days (Figure 8c) and an advancing onset of summer stratification (Figure 8d), along with the surface water warming. Using linear regression analysis, the number of stratified days increased at an average rate of 6.00 ± 3.54 d per decade ($p < 0.05$), resulting in 15 additional days in 2012 compared to 1979. Meanwhile, the onset of summer stratification advanced by an average of 4.20 ± 2.02 d per decade ($p < 0.05$), which corresponds to a change of 7 days during 1979–2012. In addition to longer-lasting and earlier stratification, the warming of Nam Co also leads to a shallowing of the thermocline depth (Figure 8e). The simulation results show that the thermocline depth declined by an average of 1.69 ± 1.36 m per decade ($p < 0.05$), or 9 m in total during 1979–2012. These simulation results for Nam Co are in accordance with many observations from temperate lakes, especially strictly dimictic lakes that freeze over each year (Arvola et al., 2010; Shimoda et al., 2011). When water temperature increased, the duration of stratification increased with earlier onset. Thermocline depth declined at the same time.

5. Driving Factors of Lake Warming

In general, air temperature is believed to be the main driver of lake surface temperature changes. Lake warming worldwide is the response of inland water bodies to global warming (O'Reilly et al., 2015; Schmid et al., 2014). Long-term observations from northern temperate lakes indicate that interannual or decadal water temperature changes also relate to climate oscillations (Adrian et al., 2009; Coats et al., 2006; Shimoda et al., 2011), such as the El Niño–Southern Oscillation (ENSO) and the Pacific Decadal Oscillation (PDO), besides global warming.

To explore possible drivers of the warming in Nam Co, linear correlation analysis was applied to summer surface water temperatures in Nam Co and climate oscillation indices, that is, ENSO, the North Atlantic Oscillation, and PDO, but the results indicate no significant relationships between them (not shown). A comparison of summer (JAS) average surface temperatures of Nam Co with annual average air temperatures on the TP (Zhang, Yao, Xie, Qin, et al., 2014) and annual land surface air temperature anomalies in the Northern Hemisphere (Jones et al., 2012) shows that all of these quantities increase with time (Figure 9a). The coefficient of correlation between the average summer surface temperatures of Nam Co and the average annual air temperatures on the TP is 0.528. It seems that warming of Lake Nam Co responded to warming air temperature. As illustrated by Figure 9a, however, there are some discrepancies between them. While regional climate warming is detected in all seasons, it is most significant in winter and least significant in summer (Kuang & Jiao, 2016; You et al., 2010). But surface water temperatures increased most in summer. So we argue that there is another forcing besides rising air temperature leading warming of Lake Nam Co. Considering the heat budget of lakes, solar radiation and longwave radiation are two main heat sources (Hipsey et al., 2014). However, the measured data for the TP show that shortwave radiation has decreased since 1984, and the rate of decrease during summer (−7 W/m^2 per decade) is most significant (Shi & Liang, 2013). In contrast, the average annual downward longwave radiation over the TP increased by 2.5 W/m^2 per decade, with the maximum increasing trend occurring in summer (5.3 W/m^2 per decade) (Shi & Liang, 2013). Based on heat budget analysis, longwave radiation contributes substantially to the heat budgets of lakes (Fink et al., 2014). In some cases, it has a close relationship with the surface warming of lakes (Arhonditsis et al., 2004). Therefore, we believe that the second forcing is the longwave radiation.

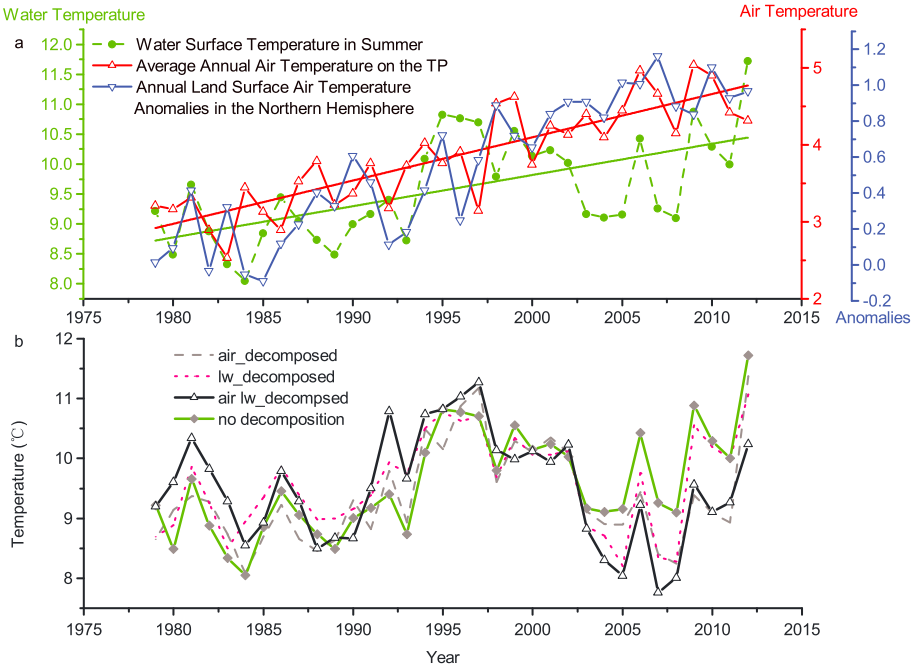

Figure 9. Causation analysis for lake warming. (a) Simulated average surface water temperature in summer (JAS), average annual air temperatures on the TP, based on 95 CMA stations, and annual land surface air temperature anomalies in the Northern Hemisphere; (b) simulated average surface water temperatures in summer (JAS) during 1979–2012 in three sensitivity experiments and the control experiment without decomposition on the forcing data. The data from the CMA stations were obtained from Zhang, Yao, Xie, Qin, et al. (2014).

To further test the roles of air temperature and longwave radiation in lake warming, we apply a decomposition method (Kendall & Stuart, 1983) using the R software package (R Core Team, 2016) to remove long-term trends from time series of air temperature and longwave radiation. Then three sensitivity experiments are conducted: (i) GLM air_decomposed, where the GLM is driven by forcing but long-term trend is removed from air temperature, and (ii) GLM lw_decomposed, where long-term trend is removed from longwave radiations, and (iii) GLM air lw_decomposed, where long-term trends are removed from both air temperature and longwave radiations. In the GLM air_decomposed experiment, the trend in average surface water temperatures during JAS is 0.23 ± 0.14°C per decade (Figure 9b). In the GLM lw_decomposed experiment, the trend becomes 0.21 ± 0.13°C per decade, and the linear regression slope is not significantly different from 0 ($p < 0.05$) (Figure 9b). The trend is 0.52 ± 0.25°C per decade when GLM is driven by the forcing data without decomposition. Therefore, both decomposed air temperature and longwave radiation lead to a shrink warming trend of surface water temperatures. In the GLM air lw_decomposed experiment, the increasing trend disappears and becomes −0.11 ± 0.16°C per decade with the linear regression slope insignificantly different from 0 ($p < 0.05$). This means that combining effect of decomposed air temperature and longwave leads the disappearance of increasing trend for water temperature. So we conclude that air temperature and longwave radiation are two driving factors that induce lake warming in the past three decades.

6. Conclusions

The validation and calibration performed in this study indicate that GLM is suitable for lake thermal simulation on the TP and at sites with elevations over 4,000 m. Driven by the corrected ITPCAS forcing data, GLM simulates the water temperatures of Nam Co from 1979 to 2012 quite well. During the summer (JAS) seasons of the last three decades, the epilimnion of Nam Co has warmed, while the onset of summer stratification advanced and the thermocline depth declined. These phenomena, as simulated by GLM, are quite coincident with observations from other temperate lakes. Increases in air temperature and longwave radiation are two driving factors responsible for the warming of Nam Co in summer.

Our research demonstrates the applicability of GLM under extreme environmental conditions. This study also indicates the possible responses of Nam Co in the context of future climate warming. Future work should

focus on the significance of these thermal changes for lake biological systems. Such studies have rarely been performed in the Tibetan Plateau until now.

Acknowledgments

We are very grateful to Shichang Kang, Yaoming Ma, and Guoshuai Zhang from the Nam Co research station for providing the meteorological data. We also thank Lazhu for providing the ITPCAS reanalysis data and the MODIS_LST data. Our colleagues' support in the field work is greatly appreciated. We would like to acknowledge the U.S. National Aeronautics and Space Administration (NASA) and U.S. Geological Survey (USGS) for making MODIS data available. Thank GLM team for making this model publicly accessible and H. Haario for sharing MCMC toolbox on the internet. The authors also thank the anonymous reviewers for their valuable comments and criticisms. This work was jointly financed by the Chinese Academy of Sciences (grant XDB03030000), the Ministry of Science and Technology of the People's Republic of China (grant 2012CB956100), the National Natural Science Foundation of China (grant 41571189), and the CADY project funded by Bundesministerium für Bildung und Forschung, Germany (grant TP2:03G0813F). Data of the figures are presented in the supporting information.

References

Adrian, R., O'Reilly, C. M., Zagarese, H., Baines, S. B., Hessen, D. O., Keller, W., … Winder, M. (2009). Lakes as sentinels of climate change. *Limnology and Oceanography*, *54*(6part2), 2283–2297. https://doi.org/10.4319/lo.2009.54.6_part_2.2283

Arhonditsis, G. B., Brett, M. T., DeGasperi, C. L., & Schindler, D. E. (2004). Effects of climatic variability on the thermal properties of Lake Washington. *Limnology and Oceanography*, *49*(1), 256–270. https://doi.org/10.4319/lo.2004.49.1.0256

Arvola, L., George, G., Livingstone, D. M., Järvinen, M., Blenckner, T., Dokulil, M. T., … Weyhenmeyer, G. A. (2010). The impact of the changing climate on the thermal characteristics of lakes. In G. George (Ed.), *The impact of climate change on European lakes* (pp. 85–101). Dordrecht, Netherlands: Springer. https://doi.org/10.1007/978-90-481-2945-4_6

Chen, Y. Y., Yang, K., He, J., Qin, J., Shi, J. C., Du, J. Y., & He, Q. (2011). Improving land surface temperature modeling for dry land of China. *Journal of Geophysical Research*, *116*, D20104. https://doi.org/10.1029/2011JD015921

Coats, R., Perez-Losada, J., Schladow, G., Richards, R., & Goldman, C. (2006). The warming of Lake Tahoe. *Climatic Change*, *76*(1-2), 121–148. https://doi.org/10.1007/s10584-005-9006-1

Crawford, T. M., & Duchon, C. E. (1999). An improved parameterization for estimating effective atmospheric emissivity for use in calculating daytime downwelling long-wave radiation. *Journal of Applied Meteorology*, *38*(4), 474–480. https://doi.org/10.1175/1520-0450(1999)038%3C0474:AIPFEE%3E2.0.CO;2

Fink, G., Schmid, M., Wahl, B., Wolf, T., & Wuest, A. (2014). Heat flux modifications related to climate-induced warming of large European lakes. *Water Resources Research*, *50*(3), 2072–2085. https://doi.org/10.1002/2013WR014448

Haario, H., Laine, M., Mira, A., & Saksman, E. (2006). DRAM: Efficient adaptive MCMC. *Statistics and Computing*, *16*(4), 339–354. https://doi.org/10.1007/s11222-006-9438-0

Hampton, S. E., Izmest'eva, L. R., Moore, M. V., Katz, S. L., Dennis, B., & Silow, E. A. (2008). Sixty years of environmental change in the world's largest freshwater lake—Lake Baikal, Siberia. *Global Change Biology*, *14*(8), 1947–1958. https://doi.org/10.1111/j.1365-2486.2008.01616.x

Hartmann, D. L., Klein Tank, A. M. G., Rusticucci, M., Alexander, L., Brönnimann, S., Charabi, Y., … Zhai, P. M. (2013). Observations: Atmosphere and surface. In T. F. Stocker, et al. (Eds.), *Climate Change 2013: The Physical Science Basis. Contribution of Working Group I to the Fifth Assessment Report of the Intergovernmental Panel on Climate Change* (pp. 159–254). Cambridge, United Kingdom and New York, NY: Cambridge University Press. https://doi.org/10.1017/CBO9781107415324.008

He, J. (2010), Development of a surface meteorological dataset of China with high temporal and spatial resolution [in Chinese], Master Dissertation, Institute of Tibetan Plateau Research, Chinese Academy of Science.

Hipsey, M. R., L. C. Bruce, and D. P. Hamilton (2014), GLM—General Lake Model: Model overview and user information. AED Report 26, (p. 42). Perth, Australia: The University of Western Australia.

Huang, L., Wang, J., Zhu, L., Ju, J., Wang, Y., & Ma, Q. (2015). Water temperature and characteristics of thermal stratification in Nam Co, Tibet (Chinese with English abstract). *Journal of Lake Science*, *27*(4), 711–718.

Immerzeel, W. W., van Beek, L. P. H., & Bierkens, M. F. P. (2010). Climate change will affect the Asian water towers. *Science*, *328*(5984), 1382–1385. https://doi.org/10.1126/science.1183188

Janssen, A. B. G., Arhonditsis, G. B., Beusen, A., Bolding, K., Bruce, L., Bruggeman, J., … Mooij, W. M. (2015). Exploring, exploiting and evolving diversity of aquatic ecosystem models: A community perspective. *Aquatic Ecology*, *49*(4), 513–548. https://doi.org/10.1007/s10452-015-9544-1

Jones, P. D., Lister, D. H., Osborn, T. J., Harpham, C., Salmon, M., & Morice, C. P. (2012). Hemispheric and large-scale land-surface air temperature variations: An extensive revision and an update to 2010. *Journal of Geophysical Research*, *117*, D05127. https://doi.org/10.1029/2011JD017139

Ke, C. Q., Tao, A. Q., & Jin, X. (2013). Variability in the ice phenology of Nam Co Lake in central Tibet from scanning multichannel microwave radiometer and special sensor microwave/imager: 1978 to 2013. *Journal of Applied Remote Sensing*, *7*(1). https://doi.org/10.1117/1.Jrs.7.073477

Kendall, M., & Stuart, A. (1983). *The advanced theory of statistics* (pp. 410–414). London: Griffin.

Kuang, X. X., & Jiao, J. J. (2016). Review on climate change on the Tibetan Plateau during the last half century. *Journal of Geophysical Research: Atmospheres*, *121*, 3979–4007. https://doi.org/10.1002/2015JD024728

Lazhu, K., Yang, J., Wang, B., Lei, Y. B., Chen, Y. Y., Zhu, L. P., … Qin, J. (2016). Quantifying evaporation and its decadal change for Lake Nam Co, central Tibetan Plateau. *Journal of Geophysical Research: Atmospheres*, *121*, 7578–7591. https://doi.org/10.1002/2015JD024523

Liu, J. S., Wang, S. Y., Yu, S. M., Yang, D. Q., & Zhang, L. (2009). Climate warming and growth of high-elevation inland lakes on the Tibetan Plateau. *Global and Planetary Change*, *67*(3-4), 209–217. https://doi.org/10.1016/j.gloplacha.2009.03.010

MacKay, M. D., Neale, P. J., Arp, C. D., de Senerpont Domis, L. N., Fang, X., Gal, G., … Stokesr, S. L. (2009). Modeling lakes and reservoirs in the climate system. *Limnology and Oceanography*, *54*(6part2), 2315–2329. https://doi.org/10.4319/lo.2009.54.6_part_2.2315

Nima, C., Hamre, B., Frette, Ø., Erga, S. R., Chen, Y. C., Zhao, L., … Stamnes, J. J. (2016). Impact of particulate and dissolved material on light absorption properties in a High-Altitude Lake in Tibet, China. *Hydrobiologia*, *768*(1), 63–79. https://doi.org/10.1007/s10750-015-2528-2

O'Reilly, C. M., Sharma, S., Gray, D. K., Hampton, S. E., Read, J. S., Rowley, R. J., … Zhang, G. (2015). Rapid and highly variable warming of lake surface waters around the globe. *Geophysical Research Letters*, *42*, 10,773–10,781. https://doi.org/10.1002/2015GL066235

Peeters, F., Livingstone, D. M., Goudsmit, G. H., Kipfer, R., & Forster, R. (2002). Modeling 50 years of historical temperature profiles in a large central European lake. *Limnology and Oceanography*, *47*(1), 186–197. https://doi.org/10.4319/lo.2002.47.1.0186

Perroud, M., Goyette, S., Martynov, A., Beniston, M., & Anneville, O. (2009). Simulation of multiannual thermal profiles in deep Lake Geneva: A comparison of one-dimensional lake models. *Limnology and Oceanography*, *54*(5), 1574–1594. https://doi.org/10.4319/lo.2009.54.5.1574

Pinker, R. T., & Laszlo, I. (1992). Modeling surface solar irradiance for satellite applications on a global scale. *Journal of Applied Meteorology*, *31*(2), 194–211. https://doi.org/10.1175/1520-0450(1992)031%3C0194:MSSIFS%3E2.0.CO;2

Qu, B., Kang, S., Chen, F., Zhang, Y., & Zhang, G. (2012). Lake ice and its effect factors in the Nam Co basin, Tibetan Plateau (Chinese with English abstract). *Progressus Inquisitiones de Mutatione Climatis*, *8*(5), 327–333.

Read, J. S., Hamilton, D. P., Jones, I. D., Muraoka, K., Winslow, L. A., Kroiss, R., … Gaiser, E. (2011). Derivation of lake mixing and stratification indices from high-resolution lake buoy data. *Environmental Modelling and Software*, *26*(11), 1325–1336. https://doi.org/10.1016/j.envsoft.2011.05.006

Read, J. S., Winslow, L. A., Hansen, G. J. A., Van den Hoek, J., Hanson, P. C., Bruce, L. C., & Markfort, C. D. (2014). Simulating 2368 temperate lakes reveals weak coherence in stratification phenology. *Ecological Modelling*, *291*, 142–150. https://doi.org/10.1016/j.ecolmodel.2014.07.029

Savtchenko, A., Ouzounov, D., Ahmad, S., Acker, J., Leptoukh, G., Koziana, J., & Nickless, D. (2004). Terra and aqua MODIS products available from NASA GES DAAC. *Advances in Space Research*, *34*(4), 710–714. https://doi.org/10.1016/j.asr.2004.03.012

Schindler, D. W. (2009). Lakes as sentinels and integrators for the effects of climate change on watersheds, airsheds, and landscapes. *Limnology and Oceanography*, *54*(6part2), 2349–2358. https://doi.org/10.4319/lo.2009.54.6_part_2.2349

Schmid, M., Hunziker, S., & Wuest, A. (2014). Lake surface temperatures in a changing climate: A global sensitivity analysis. *Climatic Change*, *124*(1-2), 301–315. https://doi.org/10.1007/s10584-014-1087-2

Schneider, P., & Hook, S. J. (2010). Space observations of inland water bodies show rapid surface warming since 1985. *Geophysical Research Letters*, *37*, L22405. https://doi.org/10.1029/2010GL045059

Sharma, S., Gray, D. K., Read, J. S., O'Reilly, C. M., Schneider, P., Qudrat, A., … Woo, K. H. (2015). A global database of lake surface temperatures collected by in situ and satellite methods from 1985–2009. *Scientific Data*, *2*, 150,008. https://doi.org/10.1038/sdata.2015.8

Sheffield, J., Goteti, G., & Wood, E. F. (2006). Development of a 50-year high-resolution global dataset of meteorological forcings for land surface modeling. *Journal of Climate*, *19*(13), 3088–3111. https://doi.org/10.1175/JCLI3790.1

Shi, Q. Q., & Liang, S. L. (2013). Characterizing the surface radiation budget over the Tibetan Plateau with ground-measured, reanalysis, and remote sensing data sets: 2. Spatiotemporal analysis. *Journal of Geophysical Research: Atmospheres*, *118*, 8921–8934. https://doi.org/10.1002/jgrd.50719

Shimoda, Y., Azim, M. E., Perhar, G., Ramin, M., Kenney, M. A., Sadraddini, S., … Arhonditsis, G. B. (2011). Our current understanding of lake ecosystem response to climate change: What have we really learned from the north temperate deep lakes? *Journal of Great Lakes Research*, *37*(1), 173–193. https://doi.org/10.1016/j.jglr.2010.10.004

Tanentzap, A. J., Hamilton, D. P., & Yan, N. D. (2007). Calibrating the Dynamic Reservoir Simulation Model (DYRESM) and filling required data gaps for one-dimensional thermal profile predictions in a boreal lake. *Limnology and Oceanography: Methods*, *5*(12), 484–494. https://doi.org/10.4319/lom.2007.5.484

Team, R. C. (2016). R: A language and environment for statistical computing. R Foundation for Statistical Computing, Vienna, Austria. Retrieved from https://www.r-project.org/

Wang, J. B., Zhu, L. P., Daut, G., Ju, J. T., Lin, X., Wang, Y., & Zhen, X. L. (2009). Investigation of bathymetry and water quality of Lake Nam Co, the largest lake on the central Tibetan Plateau, China. *Limnology*, *10*(2), 149–158. https://doi.org/10.1007/s10201-009-0266-8

Yang, K., He, J., Tang, W. J., Qin, J., & Cheng, C. C. K. (2010). On downward shortwave and longwave radiations over high altitude regions: Observation and modeling in the Tibetan Plateau. *Agricultural and Forest Meteorology*, *150*(1), 38–46. https://doi.org/10.1016/j.agrformet.2009.08.004

Yang, R., Zhu, L., Wang, J., Ju, J., Ma, Q., Turner, F., & Guo, Y. (2017). Spatiotemporal variations in volume of closed lakes on the Tibetan Plateau and their climatic responses from 1976 to 2013. *Climatic Change*, *140*(3-4), 621–633. https://doi.org/10.1007/s10584-016-1877-9

Yao, H., Samal, N. R., Joehnk, K. D., Fang, X., Bruce, L. C., Pierson, D. C., … James, A. (2014). Comparing ice and temperature simulations by four dynamic lake models in Harp Lake: Past performance and future predictions. *Hydrological Processes*, *28*(16), 4587–4601. https://doi.org/10.1002/hyp.10180

You, Q. L., Kang, S. C., Pepin, N., Flugel, W. A., Sanchez-Lorenzo, A., Yan, Y. P., & Zhang, Y. J. (2010). Climate warming and associated changes in atmospheric circulation in the eastern and central Tibetan Plateau from a homogenized dataset. *Global and Planetary Change*, *72*(1-2), 11–24. https://doi.org/10.1016/j.gloplacha.2010.04.003

Zhang, G. Q., Yao, T. D., Xie, H. J., Qin, J., Ye, Q. H., Dai, Y. F., & Guo, R. F. (2014). Estimating surface temperature changes of lakes in the Tibetan Plateau using MODIS LST data. *Journal of Geophysical Research: Atmospheres*, *119*, 8552–8567. https://doi.org/10.1002/2014JD021615

Zhang, G. Q., Yao, T. D., Xie, H. J., Zhang, K. X., & Zhu, F. J. (2014). Lakes' state and abundance across the Tibetan Plateau. *Chinese Science Bulletin*, *59*(24), 3010–3021. https://doi.org/10.1007/s11434-014-0258-x

Zhou, S. Q., Kang, S. C., Chen, F., & Joswiak, D. R. (2013). Water balance observations reveal significant subsurface water seepage from Lake Nam Co, south-central Tibetan Plateau. *Journal of Hydrology*, *491*, 89–99. https://doi.org/10.1016/j.jhydrol.2013.03.030